

# Northumbria Research Link

Citation: Eltokhey, Mahmoud Wafik, Khalighi, Mohammad-Ali and Ghassemlooy, Fary (2020) Dimming-Aware Interference Mitigation for NOMA-Based Multi-Cell VLC Networks. IEEE Communications Letters, 24 (11). pp. 2541-2545. ISSN 1089-7798

Published by: IEEE

URL: <https://doi.org/10.1109/LCOMM.2020.3007552> <<https://doi.org/10.1109/LCOMM.2020.3007552>>

This version was downloaded from Northumbria Research Link:  
<http://nrl.northumbria.ac.uk/id/eprint/44998/>

Northumbria University has developed Northumbria Research Link (NRL) to enable users to access the University's research output. Copyright © and moral rights for items on NRL are retained by the individual author(s) and/or other copyright owners. Single copies of full items can be reproduced, displayed or performed, and given to third parties in any format or medium for personal research or study, educational, or not-for-profit purposes without prior permission or charge, provided the authors, title and full bibliographic details are given, as well as a hyperlink and/or URL to the original metadata page. The content must not be changed in any way. Full items must not be sold commercially in any format or medium without formal permission of the copyright holder. The full policy is available online: <http://nrl.northumbria.ac.uk/policies.html>

This document may differ from the final, published version of the research and has been made available online in accordance with publisher policies. To read and/or cite from the published version of the research, please visit the publisher's website (a subscription may be required.)



**Northumbria**  
**University**  
NEWCASTLE

# Dimming-Aware Interference Mitigation for NOMA-Based Multi-Cell VLC Networks

Mahmoud Wafik Eltokhey, *Member, IEEE*, Mohammad-Ali Khalighi<sup>1b</sup>, *Senior Member, IEEE*, and Zabih Ghassemlooy<sup>2</sup>, *Senior Member, IEEE*

**Abstract**—This letter proposes inter-cell interference mitigation in a dimming-aware way for multi-cell visible-light communication networks, through efficient time-scheduling, scaling, and coordination of non-orthogonal multiple access (NOMA) transmissions at the access points. By this method, users are grouped and served in different time slots depending on whether they are at the center or at the edge of the cell. This reduces the number of NOMA users per time slot, which decreases the network computational complexity, by reducing the average number of successive interference cancellation steps. Comparison of the proposed scheme with the classical NOMA over different dimming constraints shows an improvement of up to 39% and 37% in the average sum-rate and fairness, respectively, for a 30% duty cycle transmission in a 4-cell scenario with 8 users.

**Index Terms**—Visible light communications, multi-cell networks, non-orthogonal multiple access, inter-cell interference.

## I. INTRODUCTION

VISIBLE-LIGHT communications (VLCs) have been receiving increasing attention for more than two decades, in particular, for providing wireless connectivity in indoor environments. The main factors driving this growing interest include the huge available bandwidth, immunity against radio-frequency (RF) induced interference, and inherent security [1]. For relatively large indoor spaces, multiple light emitting diode (LED) luminaires serve as access points (APs), which handle users in their coverage area, forming hence a multi-cell VLC network. There, users can be classified as cell-center or cell-edge users (CCUs or CEUs, respectively), depending on coverage by one or more APs. In such networks, the performances of CCUs are affected by inter-user interference (IUI), resulting from signals of users being in the same cell, whereas CEUs should mitigate both IUI and inter-cell interference (ICI), the latter resulting from signals of users in the neighboring cells. This reflects the importance of employing efficient multiple-access (MA) techniques in minimizing IUI and ICI effects.

Focusing on downlink transmission within this context, one popular scheme is the power-domain non-orthogonal

MA (NOMA). By this scheme that we will call simply NOMA, the APs (i.e., the transmitters, Tx) multiplex users' signals in the power domain using superposition coding. At the user side (i.e., the receiver, Rx), to minimize multi-user interference (MUI), successive interference cancellation (SIC) is performed [2]. The particular interest of NOMA signaling in VLC networks arises from several facts: (i) APs typically need to handle a relatively small number of users, hence, requiring a small number of SIC detection steps; (ii) the limited mobility of users in indoor VLC scenarios and the overall slow channel time variations makes acquiring the users' channel state information (CSI) for SIC detection rather easy; (iii) the limited link distance enables signal detection at relatively high average signal-to-noise ratios (SNRs) [3]. In addition, the advantage of NOMA over orthogonal MA techniques has been demonstrated in several previous works, e.g., [4], [5].

There is an apparent need for reducing the number of users in SIC detection. The reason is two fold: (i) the users with higher decoding orders (i.e., lower detection priority) require CSI of the preceding users; (ii) the users with lower decoding orders suffer from MUI arising from the higher decoding-order users. In this letter, we propose a NOMA-based scheme, called time-sliced (TS) NOMA, which adds a temporal dimension to the conventional NOMA. By TS-NOMA, CCUs and CEUs in a given cell are grouped and handled by NOMA in separate time slots. The duration and the position of these time slots are determined according to the requirements of light dimming and ICI mitigation. This solution offers reduced detection complexity and decreased IUI, compared with the conventional NOMA, while enabling efficient ICI mitigation and light dimming. It also facilitates network real-time adaptation in the case of users mobility.

The concept of adding a temporal dimension to NOMA has also been considered for RF networks. For instance, in [6], optimized power allocation (PA) and user scheduling for NOMA were considered for massive Internet-of-Things (IoT) networks. In the context of MA mobile edge computing, [7] proposed optimized time allocation for mobile users for offloading their computational workload to edge servers using NOMA. Temporal fair user scheduling was also considered for NOMA signaling in [8]. Compared with these works, our proposed technique differs in considering dimming-compatible duty cycling of NOMA signals for multi-cell VLC networks.

## II. MAIN ASSUMPTIONS

Consider a multi-cell VLC network where a central control unit coordinates  $N_t$  APs and classifies  $N_r$  users as CCUs or CEUs. Without loss of generality, we consider

Manuscript received June 10, 2020; accepted June 30, 2020. Date of publication July 6, 2020; date of current version November 11, 2020. This work has received funding from the European Union's Horizon 2020 research and innovation programme under the Marie Skłodowska-Curie grant agreement No. 764461 (VisIoN: Visible light based Interoperability and Networking). The associate editor coordinating the review of this letter and approving it for publication was H. Le-Minh. (*Corresponding author: Mohammad-Ali Khalighi.*)

Mahmoud Wafik Eltokhey and Mohammad-Ali Khalighi are with Aix-Marseille University, CNRS, Centrale Marseille, Institut Fresnel, Marseille, France (e-mail: mahmoud.eltokhey@centrale-marseille.fr; ali.khalighi@fresnel.fr).

Zabih Ghassemlooy is with the Optical Communications Research Group, Faculty of Engineering and Environment, Northumbria University, Newcastle upon Tyne NE1 8ST, U.K. (e-mail: z.ghassemlooy@northumbria.ac.uk).

Digital Object Identifier 10.1109/LCOMM.2020.3007552

intensity modulation based on DC-biased optical orthogonal frequency-division multiplexing (DCO-OFDM). Let the  $i^{\text{th}}$  AP,  $\text{AP}_i$  serves  $N_i$  users, and denote by  $h_{ij}$  the channel gain between  $\text{AP}_i$  and the  $j^{\text{th}}$  user  $U_{ij}$  (handled by  $\text{AP}_i$ ). Assume that (i) each AP (an LED luminaire) has a Lambertian pattern; (ii) each Rx uses a PIN photo-detector (PD) with an optical concentrator; and (iii) any CEU is only associated with the AP corresponding to the strongest channel gain [9]. Accounting for line-of-sight (LOS) propagation while neglecting non-LOS contribution, the channel DC gain is given by [1]:

$$h_{ij} = \mathcal{R} \mathcal{S} \frac{(m+1) A_{ij}}{2\pi l_{ij}^2} \cos^m(\phi_{ij}) \cos(\theta_{ij}), \quad (1)$$

where  $\phi_{ij}$  is the Tx angle of emission,  $\theta_{ij}$  denotes the incident angle, and  $l_{ij}$  is the distance between  $\text{AP}_i$  and  $U_{ij}$ . Also,  $\mathcal{R}$  is the PD responsivity,  $\mathcal{S}$  and  $m$  are the LED conversion efficiency and Lambertian order, respectively, and  $A_{ij}$  is effective area of the Rx, which is given by  $A_{ij} = q^2 A_{\text{PD}} / \sin^2(\theta_{\text{FOV}})$  [1], where  $A_{\text{PD}}$  is the PD active area,  $q$  is the optical concentrator refractive index, and  $\theta_{\text{FOV}}$  is the Rx field-of-view (FOV), which are assumed to be the same for all Rxs for notation simplicity. To comply with the light dimming requirement, we set the duty cycle  $\delta$  of the LED emission to  $\delta = \tau/T$ , where  $\tau$  is the signal transmission time over a certain period  $T$  [10]. Denoting by  $P_o(t) > 0$  the LED output optical power, we define the dimming ratio  $\gamma$  as:

$$\gamma = \frac{1}{P} \lim_{T \rightarrow \infty} \frac{1}{T} \int_0^T P_o(t) dt, \quad 0 \leq \gamma \leq 1 \quad (2)$$

where  $P$  is the average LED optical power in the case of no dimming, i.e., for  $\gamma = 1$ . The dimming ratio  $\gamma$  (in power domain) is related to the duty cycle  $\delta$  (in time domain). Note that such a dimming control by duty cycling the transmitted signal can also be applied to DCO-OFDM signaling [11], [12]. In this case, the signal can be modeled as a zero-mean Gaussian random process based on the central limit theorem [13], hence, dimming is mainly controlled by the DC bias.

### III. CONVENTIONAL NOMA SIGNALING

At the Tx (i.e., the AP), NOMA users signals are multiplexed in the power domain using superposition coding. The assigned power to each user is set according to a PA scheme and its channel gain; users with higher channel gains are allocated less power. At the Rx, SIC detection is performed, where users with larger channel gains decode their signal in higher orders (IUI of lower order users being ideally eliminated by SIC [3]). Assuming perfect CSI knowledge for all users, after excluding the DC component, the received signal by  $U_{ij}$  from  $\text{AP}_i$  is given by:

$$r_{ij} = a_{ij} \sqrt{P_e} h_{ij} d_{ij} + \sum_{k=1}^{j-1} a_{ik} \sqrt{P_e} h_{ij} d_{ik} + \sum_{k=j+1}^{N_i} a_{ik} \sqrt{P_e} h_{ij} d_{ik} + z_j, \quad (3)$$

where  $P_e$  and  $a_{ij}$  represent the total transmit electrical power (excluding the DC offset) and the corresponding PA weight,

respectively, where  $P_o = \mathcal{S} \sqrt{P_e}$ . Also,  $d_{ij}$  is the desired data and  $z_j$  denotes the Gaussian noise with variance  $\sigma_n^2$ . The first, second, and third terms in (3) represent the desired signal, the suppressed interference by SIC, and the residual interference, respectively. For the sake of simplicity and without loss of generality, we consider static PA such that  $a_{ij}^2 = \alpha a_{ij-1}^2$ , where  $0 < \alpha < 1$  represents the PA factor, i.e., the ratio between the power level of  $U_{ij}$  to that of  $U_{ij-1}$  (the preceding user in the decoding order) [3]. To ensure normalized  $P_e$ , we set  $\sum_{j=1}^{N_i} a_{ij}^2 = 1$ . The electrical signal-to-interference-plus-noise ratio (SINR) for  $U_{ij}$  is then calculated as:

$$\text{SINR}_{\text{NOMA}, U_{ij}} = \frac{h_{ij}^2 P_e a_{ij}^2}{I_{\text{ICI}} + h_{ij}^2 P_e \sum_{k>j} a_{ik}^2 + \sigma_n^2}, \quad (4)$$

where  $I_{\text{ICI}}$  denotes the ICI power. The upper bound on the achievable rate of  $U_{ij}$  in terms of the duty cycle  $\delta$ , corresponding to a dimming ratio of  $\gamma$ , is given as:

$$R_{\text{NOMA}, U_{ij}} = \delta \frac{B}{2} \log_2 (1 + \text{SINR}_{\text{NOMA}, U_{ij}}) \quad (\text{bps}), \quad (5)$$

where  $B$  is the system bandwidth and the division by the factor 2 is due to Hermitian symmetry constraint of DCO-OFDM.

## IV. TS-NOMA SIGNALING

### A. Concept

The idea behind TS-NOMA is to adjust the duty cycle of the NOMA signal at the APs to eliminate ICI and to satisfy the light dimming requirement. Firstly, at the central control unit, users are classified as CCU or CEU depending on their channel gains. Afterwards, at each AP, NOMA is applied separately to signals of CEUs and CCUs, which are then transmitted in two different time slots, such that the duty cycle of the total transmission time satisfies the dimming requirement. In addition, CEU signals are transmitted in different non-overlapping time slots to guarantee no ICI. To clarify better the idea, consider the example of Fig. 1(a) where a 4-cell VLC network is shown with the AP positioned at the center of each cell, and two CCUs within each cell and two CEUs in the intersecting areas of adjacent cells. Note that we define the cell boundaries based on the users' CSI, according to a predefined threshold for channel gain [9], which is set here to  $9.74 \times 10^{-7}$ , corresponding to a cell radius of 2 m.

Here, we consider two schemes: (i) Scheme A, see Fig. 1(b), where in addition to separating CEU signals in time, all CCU signals (from different APs) are transmitted in non-overlapping time slots; and (ii) Scheme B, see Fig. 1(c), where the same time slot is attributed to the CCUs in different cells. The choice between these two schemes depends on the dimming requirement (see Subsection IV-B). In Fig. 1,  $d_{ij}$  denotes the signal of  $U_{ij}$ , and  $t_{c,i}$  and  $t_{e,i}$  refer to the time slots attributed to CCU and CEU groups served by  $\text{AP}_i$ , respectively.

We denote by  $c_{\text{int}}$  the number of coordinating APs, having intersecting coverage areas;  $c_{\text{int}} = 4$  in the example of Fig. 1. To mitigate ICI, the transmission cycle  $T$  is divided among the  $c_{\text{int}}$  APs: each AP disposing of an interval of  $T/c_{\text{int}}$  for signal transmission, where the maximum duty cycle is  $\delta_{\text{max}} = 1/c_{\text{int}}$ . Note that, as CCUs are not affected by ICI, their signals

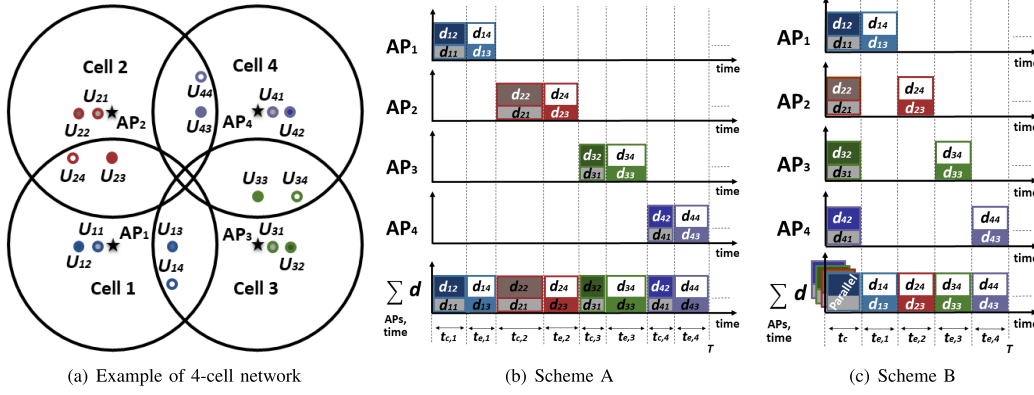


Fig. 1. Illustration of the proposed TS-NOMA schemes. (a): top view of a 4-cell network example. (b) and (c): signal transmission timing for different users according to Scheme A and B, respectively.

could be transmitted in parallel by all the APs, as considered in Fig. 1(c). However, in this case, they must use the same  $t_{c,i}$ , hence having less flexibility, as compared with Fig. 1(b).

Lets  $N_{c,i}$  and  $N_{e,i}$  denote the numbers of CCUs and CEUs served by  $AP_i$ , respectively. Assuming perfect synchronization and excluding the DC signal component, the received signal for  $CCU_j$  handled by  $AP_i$  over time slot  $t_{c,i}$  is:

$$r_{ij}(t) = a_{ij} \sqrt{P_e} h_{ij} d_{ij} + \sum_{k=1}^{j-1} a_{ik} \sqrt{P_e} h_{ij} d_{ik} + \sum_{k=j+1}^{N_{c,i}} a_{ik} \sqrt{P_e} h_{ij} d_{ik} + z_j. \quad (6)$$

Similarly, for  $CEU_j$  served by  $AP_i$  in time slot  $t_{e,i}$  we have:

$$r_{ij}(t) = a_{ij} \sqrt{P_e} h_{ij} d_{ij} + \sum_{k=1}^{j-1} a_{ik} \sqrt{P_e} h_{ij} d_{ik} + \sum_{k=j+1}^{N_{e,i}} a_{ik} \sqrt{P_e} h_{ij} d_{ik} + z_j. \quad (7)$$

For both cases, the corresponding SINR is given by:

$$\text{SINR}_{\text{TS},U_{ij}} = \frac{h_{ij}^2 P_e a_{ij}^2}{h_{ij}^2 P_e \sum_{k>j} a_{ik}^2 + \sigma_n^2}, \quad (8)$$

and the approximate maximum achievable throughput is then:

$$R_{\text{TS},U_{ij}} = \delta_i \frac{B}{2} \log_2 (1 + \text{SINR}_{\text{TS},U_{ij}}) \quad (\text{bps}), \quad (9)$$

where  $\delta_i$  is the transmission duty cycle for  $U_{ij}$  corresponding to  $AP_i$ . Note that,  $\delta_i = t_{c,i}/T$  if  $U_{ij}$  is a CCU, and  $\delta_i = t_{e,i}/T$  if it is a CEU. Also,  $(t_{c,i} + t_{e,i})/T = \delta$ .

## B. TS-NOMA Schemes

We consider three cases for the transmission scheme, depending on the required duty cycle  $\delta$ . Note that we reasonably assume the same dimming level for all APs.

1) *No Dimming*,  $\delta = 1$ : In this case, we can use either Scheme A or B. However, to maximize network capacity, parallel transmission of CCUs signals is preferred, i.e., by Scheme B, Fig. 1(c). Note that, (i) in the intervals where no “signal” is transmitted, the corresponding APs still transmit

the DC bias to ensure lighting; (ii) in case where there is no CEU in a cell, the corresponding CEU time slot is devoted to the transmission of CCU signals in all cells; and (iii) the absence of CCUs in a cell does not change the timing in order to avoid ICI with CCU signals from the other cells.

2)  $\delta > \delta_{\max}$ : In this case,  $\delta$  cannot be satisfied using Scheme A because this latter can guarantee dimming with no ICI only for  $\delta \leq \delta_{\max}$ . Using Scheme B, we transmit the signals of CCUs (which do not suffer from ICI) in parallel from all APs. This way, the time intervals for non-overlapping transmission of CEU signals can be increased. We have,  $t_{c,i} + \sum_{i=1}^{c_{\text{int}}} t_{e,i} = T$ . For simplicity, we consider the same  $t_{e,i}$  for all APs. Since for dimming constraint we have  $(t_{c,i} + t_{e,i})/T = \delta$ , therefore:

$$\begin{cases} \delta_i = (1 - \delta)/(c_{\text{int}} - 1) & \text{for CEUs,} \\ \delta_i = (\delta c_{\text{int}} - 1)/(c_{\text{int}} - 1) & \text{for CCUs.} \end{cases} \quad (10)$$

Note, in the absence of CEUs in a cell, the corresponding time slot is used by the CCUs in the same cell to comply with the dimming condition for all APs. If there is no CCU in a cell, the timing is still not changed to avoid ICI with CCU signals from the other cells.

3)  $\delta \leq \delta_{\max}$ : Here, the required dimming condition can be satisfied by both Schemes A and B. However, as there is no room to increase the network capacity by improving time resources utilization, sequential transmission of CCU signals is preferred, i.e., Scheme A. This allows allocating different durations for  $t_{c,i}$ , thus more flexibility in timing design. If there is no CEU (CCU) in a cell, the corresponding time slot is used by the CCUs (CEUs) in the same cell.

## C. Time-Slot Fixing Strategies

For setting the different time intervals  $t_{c,i}$  and  $t_{e,i}$  for CCUs and CEUs, we consider six specific strategies that we will refer to as S1 to S6, as described in the following.

- 1) TS-NOMA-S1: As the simplest way, for all  $i$ , we use equal time slots, i.e.,  $t_{c,i} = t_{e,i}$ .
- 2) TS-NOMA-S2: We set slot durations according to the associated number of users. For Scheme A, Fig. 1(b), this results in  $t_{c,i} = N_{c,i}/N_i$  and  $t_{e,i} = N_{e,i}/N_i$ . For Scheme B, Fig. 1(c),  $t_{e,i}$  is determined by  $N_{e,i}$ , whereas  $t_c$  is set considering the maximum number of CCUs  $N_{c,\max}$  per group among all CCU groups, i.e.,  $N_{c,\max} =$



$\max(N_{c,1}, \dots, N_{c,N_t})$ . This ensures setting the largest possible  $t_c$ . We have then  $t_c = N_{c,\max}/(N_{c,\max} + \sum_{i=1}^{N_t} N_{e,i})$  and  $t_{e,i} = N_{e,i}/(N_{c,\max} + \sum_{i=1}^{N_t} N_{e,i})$ .

- 3) TS-NOMA-S3: We set  $t_{c,i}$  and  $t_{e,i}$  according to the average channel gain for each group of CCUs and CEUs (similar to the idea of static PA in NOMA [3]). This way, for a larger average channel gain, we allocate a smaller duration to the corresponding time slot. The ratio between each two consecutive time slots  $\zeta$  is a constant, called time allocation (TA) coefficient. This allows time slot allocation to be better tailored to the channel gains in every group. For Scheme B,  $t_c$  is set by considering the minimum average channel gain per group (among all CCU groups), to ensure the largest possible  $t_c$ .
- 4) TS-NOMA-S4: Setting slot duration is based on the same approach as in TS-NOMA-S3, while considering as criterion the average channel gain divided by the number of users in the group. This allows groups with a large number of users to be allocated a long time slot, hence, resulting in a still better fairness in the network.
- 5) TS-NOMA-S5: This strategy applies to the case of  $\delta > \delta_{\max}$ , where we use (10) to calculate  $t_{c,i}$  and  $t_{e,i}$ , to satisfy dimming and mitigate ICI.
- 6) TS-NOMA-S6: For the case of  $\delta \leq \delta_{\max}$ , users are served as in conventional NOMA, while avoiding parallel transmission of APs (i.e., to avoid ICI).

Note that the described strategies should be selected depending on the required dimming, or in other words,  $\delta$ . For  $\delta = 1$ , TS-NOMA-S1, -S2, -S3, and -S4 can be used. For  $\delta \leq \delta_{\max}$ , these four strategies, as well as TS-NOMA-S6 can be used, where  $t_{c,i}$  and  $t_{e,i}$  are calculated separately in each cell. For  $\delta > \delta_{\max}$ , only TS-NOMA-S5 can be used. In fact, TS-NOMA-S1 to -S4 do not satisfy the constraints of dimming and ICI mitigation in this case, and therefore cannot be used.

## V. TS-NOMA PERFORMANCE

### A. Network Performance Metrics

We consider two performance metrics, i.e., the maximum achievable throughput and the *Jain's fairness index* (FI) [14]. This latter is a measure of the throughput homogeneity among users, which for a total number of  $N_r$  users is defined as:

$$FI = \left( \sum_{i=1}^{N_t} \sum_{j=1}^{N_i} R_{ij} \right)^2 / \left( N_r \sum_{i=1}^{N_t} \sum_{j=1}^{N_i} R_{ij}^2 \right), \quad (11)$$

where  $R_{ij}$  denotes the maximum achievable throughput of  $U_{ij}$ . We have  $FI = 1$  if all  $R_{ij}$  are equal; as the difference between  $R_{ij}$  increases, FI becomes smaller.

### B. Main Assumptions and Considered Scenarios

We consider a 4-cell network, as in Fig. 1(a), where APs are positioned at the center of the cells and the emitted optical power from each AP is set to  $P_o = 1.584\text{W}$  as in [14]. The considered heights of the APs and the Rxs are 2.5 and 0.85 m, respectively. Three different scenarios are considered, called Scenarios 1, 2, and 3, for which we set  $N_r$  to 8, 12, and 16, and the corresponding number of CEUs to 4, 4, and 8, respectively. These represent an increased level of IUI

TABLE I  
SIMULATION PARAMETERS

Parameter	Value
Room dimension	(7 m × 7 m × 3 m)
LED luminaire Lamertian order $m$ [14]	1
Number of LED chips per luminaire [14]	36
Maximum signal current per LED chip [14]	100 mA
LED conversion efficiency $\mathcal{S}$ [14]	0.44 W/A
PD responsivity $\mathcal{R}$ [4]	0.4 A/W
PD area $A_{\text{PD}}$ [14]	1 cm <sup>2</sup>
Rx's FOV $\theta_{\text{FOV}}$ [14]	62 deg.
Refractive index of optical concentrator $q$ [14]	1.5
BW $B$	10 MHz
Equivalent Rx noise power spectral density [4]	$10^{-21}$ A <sup>2</sup> /Hz

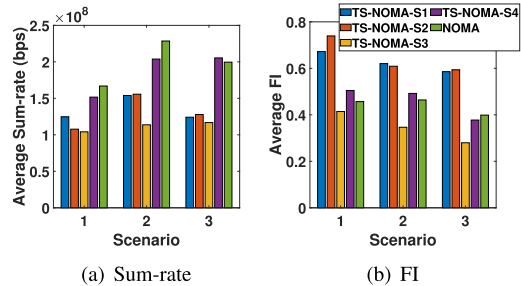


Fig. 2. Comparison of sum-rate and FI for TS-NOMA and NOMA for the case of no dimming ( $\delta = 1$ ).

and ICI in the case of conventional NOMA. For each scenario, 200 randomly generated users positions are used over which the performance is averaged.<sup>1</sup> The PA coefficient  $\alpha$  is set to 0.3, providing the best compromise between sum-rate and FI. The same value is adopted for the TA coefficient  $\zeta$ . Table I summarizes the other simulation parameters.

### C. Numerical Results

Here we compare the sum-rate and FI of TS-NOMA with conventional NOMA as shown in Fig. 2 for the case of no dimming, i.e.,  $\delta = 1$ , and the three considered scenarios described in Subsection V-B. We notice that, despite the ICI mitigation merits of TS-NOMA, NOMA achieves a better sum-rate, except for TS-NOMA-S4 case, which has a close performance to NOMA. The reason is that TS-NOMA-S1, -S2, and -S3 schemes have a poor sum-rate performance when a relatively large number of users with relatively low average channel gains are in a group, where they are allocated a relatively short time slot. The TS-NOMA-S4 strategy avoids such conditions, as described above, which results in a higher average sum-rate. As concerns FI, we notice from Fig. 2(b) that generally TS-NOMA schemes outperform conventional NOMA, except for TS-NOMA-S3, and for TS-NOMA-S4 in Scenario 3. The best FI are obtained for TS-NOMA-S1 and -S2, as expected: the former equally divides the time resources among the users, whereas the latter allocates them based on the number of users in each group. For TS-NOMA-S3 and -S4, FI is penalized by large variations in time slot durations due to considering a constant TA coefficient.

<sup>1</sup>Note that we exclude in the simulations those scenarios for which CEUs are in coverage areas of more than two APs. Indeed, for such cases, the NOMA performance will be penalized considerably because of ICI, in contrary to TS-NOMA where CEUs of each AP are served in non-overlapping time slots.

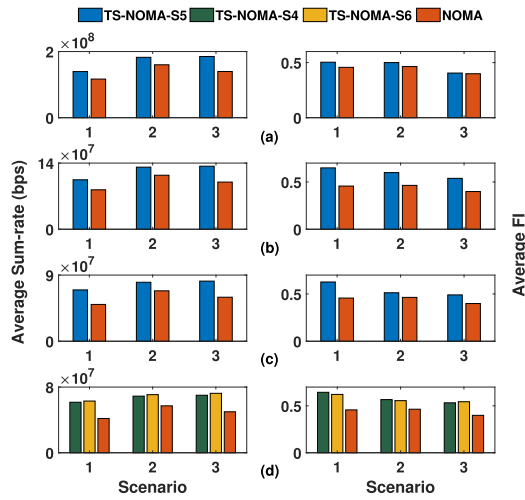


Fig. 3. Comparison of sum-rate and FI between TS-NOMA and NOMA for (a)  $\delta = 70\%$ , (b)  $50\%$ , (c)  $30\%$ , and (d)  $25\%$ .

Overall, compared with conventional NOMA, the presented results suggest TS-NOMA-S4 as the most appropriate scheme that makes a good compromise between sum-rate and FI.

Finally, Fig.3 compares TS-NOMA and NOMA over sum-rate and FI, for  $\delta < 1$ , namely  $70\%$ ,  $50\%$ ,  $30\%$ , and  $25\%$  for the three considered scenarios. Given that  $\delta_{\max} = 1/4$ , for the three former cases where  $\delta > \delta_{\max}$ , we use the TS-NOMA-S5 strategy, whereas for the last case where  $\delta = \delta_{\max}$ , we use TS-NOMA-S4 (which achieved the best sum-rate and acceptable FI in Fig.2) and TS-NOMA-S6. We notice from Figs.3(a), (b), and (c) that TS-NOMA-S5 outperforms NOMA in both sum-rate and FI in all scenarios. This superiority of TS-NOMA-S5 can be explained by the decreased IUI due to handling a smaller number of NOMA users per time interval, and the elimination of ICI. Similarly, from Fig.3(d) we notice a better sum-rate and FI for TS-NOMA-S4 and -S6, compared to conventional NOMA, due to minimized ICI. Although TS-NOMA-S6 achieves a higher sum-rate than TS-NOMA-S4 because of allocating more time resources per user, it needs the same number of SIC detection steps as for conventional NOMA. Overall, compared with conventional NOMA, we can conclude TS-NOMA-S4 and -S5 as the most appropriate schemes for  $\delta \leq \delta_{\max}$  and  $\delta > \delta_{\max}$ , respectively, providing improved sum-rate and FI, as well as reduced Rx complexity.

Note also that for all TS-NOMA schemes in Fig.3, we notice a degradation of FI from Scenario 1 to 3 (from the smallest to the largest number of users), which is because of increased IUI. In addition, we note an increase in the average sum-rate for scenarios with a larger number of users. Yet, the increase in sum-rate from Scenario 2 to 3 is less significant than that from Scenario 1 to 2. This is due to the decrease in the available time resources per user.

## VI. CONCLUDING REMARKS

We proposed the TS-NOMA scheme for multi-cell VLC networks and showed its efficiency in handling MUI, compared with the conventional NOMA. By separating in time

domain the CCUs and CEUs in different NOMA groups, the proposed TS-NOMA offers ICI mitigation, dimming compatibility, as well as reduction in the number of users handled by NOMA per time interval, thus a reduced Rx computational complexity. We showed the advantage of TS-NOMA in terms of sum-rate and network fairness, especially for the case of light dimming.

As concerns the computational complexity of TS-NOMA, the main factors are: (i) power allocation (which is negligible due to using static PA); (ii) the number of SIC operations at the Rxs (with an advantage over conventional NOMA due to handling less users per time slot); and (iii) CSI acquisition (which is the same as for NOMA). Nevertheless, using TS-NOMA increases the network complexity due to synchronization management (which is rather low due to handling only two time slots per AP) and time-slot allocation. For this latter, the highest complexity in the case of dimming corresponds to TS-NOMA-S4 for  $\delta \leq \delta_{\max}$ , which requires in the worst case  $N_{\text{CCUs}} + N_{\text{CEUs}} + c_{\text{int}} - 1$  additions and  $4 c_{\text{int}} + 1$  divisions.

Overall, the increased complexity is quite justified, given the improvement achieved in the overall network performance.

## REFERENCES

- [1] Z. Ghassemlooy, L. N. Alves, S. Zvanovec, and M. A. Khalighi, Eds., *Visible Light Communications: Theory and Applications*. Boca Raton, FL, USA: CRC Press, 2017.
- [2] Z. Ding, M. Peng, and H. V. Poor, "Cooperative non-orthogonal multiple access in 5G systems," *IEEE Commun. Lett.*, vol. 19, no. 8, pp. 1462–1465, Aug. 2015.
- [3] H. Marshoud, V. M. Kapinas, G. K. Karagiannidis, and S. Muhaidat, "Non-orthogonal multiple access for visible light communications," *IEEE Photon. Technol. Lett.*, vol. 28, no. 1, pp. 51–54, Jan. 1, 2016.
- [4] L. Yin, W. O. Popoola, X. Wu, and H. Haas, "Performance evaluation of non-orthogonal multiple access in visible light communication," *IEEE Trans. Commun.*, vol. 64, no. 12, pp. 5162–5175, Dec. 2016.
- [5] M. W. Eltokhey, M.-A. Khalighi, and Z. Ghassemlooy, "Multiple access techniques for VLC in large space indoor scenarios: A comparative study," in *Proc. 15th Int. Conf. Telecommun. (ConTEL)*, Graz, Austria, Jul. 2019, pp. 1–6.
- [6] D. Zhai, R. Zhang, L. Cai, B. Li, and Y. Jiang, "Energy-efficient user scheduling and power allocation for NOMA-based wireless networks with massive IoT devices," *IEEE Internet Things J.*, vol. 5, no. 3, pp. 1857–1868, Jun. 2018.
- [7] Y. Wu, K. Ni, C. Zhang, L. P. Qian, and D. H. K. Tsang, "NOMA-assisted multi-access mobile edge computing: A joint optimization of computation offloading and time allocation," *IEEE Trans. Veh. Technol.*, vol. 67, no. 12, pp. 12244–12258, Dec. 2018.
- [8] S. Shahsavari, F. Shirani, and E. Erkip, "A general framework for temporal fair user scheduling in NOMA systems," *IEEE J. Sel. Topics Signal Process.*, vol. 13, no. 3, pp. 408–422, Jun. 2019.
- [9] S. Feng, R. Zhang, W. Xu, and L. Hanzo, "Multiple access design for ultra-dense VLC networks: Orthogonal vs non-orthogonal," *IEEE Trans. Commun.*, vol. 67, no. 3, pp. 2218–2232, Mar. 2019.
- [10] K. Lee and H. Park, "Modulations for visible light communications with dimming control," *IEEE Photon. Technol. Lett.*, vol. 23, no. 16, pp. 1136–1138, Aug. 15, 2011.
- [11] Z. Wang, W.-D. Zhong, C. Yu, J. Chen, C. P. S. Francois, and W. Chen, "Performance of dimming control scheme in visible light communication system," *Opt. Express*, vol. 20, no. 17, pp. 18861–18868, Aug. 2012.
- [12] X. You, J. Chen, H. Zheng, and C. Yu, "Efficient data transmission using MPPM dimming control in indoor visible light communication," *IEEE Photon. J.*, vol. 7, no. 4, pp. 1–12, Aug. 2015.
- [13] R. Mesleh, H. Elgala, and H. Haas, "On the performance of different OFDM based optical wireless communication systems," *IEEE/OSA J. Opt. Commun. Netw.*, vol. 3, no. 8, pp. 620–628, Aug. 2011.
- [14] M. W. Eltokhey, M. A. Khalighi, A. S. Ghazy, and S. Hranilovic, "Hybrid NOMA and ZF pre-coding transmission for multi-cell VLC networks," *IEEE Open J. Commun. Soc.*, vol. 1, pp. 513–526, 2020.